Evaluation of Microstructure and Phase Relations in a Powder Processed Ti-44Al-12Nb Alloy

S.G. Kumar, R.G. Reddy, J. Wu, and J. Holthus

Titanium aluminides based on the ordered face-centered tetragonal γTiAl phase possess attractive properties, such as low density, high melting point, good elevated temperature strength, modulus retention, and oxidation resistance, making these alloys potential high-temperature structural materials. These alloys can be processed by both ingot metallurgy and powder metallurgy routes. In the present study, three variations of the powder metallurgy route were studied to process a Ti-44Al-12Nb (at.%) alloy: (a) cold pressing followed by reaction sintering (CP process); (b) cold pressing, vacuum hot pressing, and then sintering (HP process); and (c) arc melting, hydride-dehydride process to make the alloy powder, cold isostatic pressing, and then sintering (AM process). Microstructural and phase relations were studied by x-ray diffraction (XRD) analysis, optical microscopy, scanning electron microscopy with an energy-dispersive spectrometer (SEM-EDS), and electron probe microanalysis (EPMA). The phases identified were Ti_3Al and TiAl; an additional Nb_2Al phase was observed in the HP sample. The microstructures of CP and HP processed samples are porous and chemically inhomogeneous whereas the AM processed sample revealed fine equiaxed microstructure. This refinement of the microstructure is attributed to the fine, homogeneous powder produced by the hydride-dehydride process and the high compaction pressures.

Keywords
microstructure, phase relations, powder metallurgy, titanium alloy

1. Introduction

INTERMETALLIC aluminides based on nickel, iron, and titanium are fast emerging as potential alternative high-temperature materials to nickel-based superalloys. These alloys possess many of the properties required to meet the ever increasing performance levels of the aerospace industry, such as high specific strength, high specific modulus, and high-temperature properties like strength, modulus retention, oxidation resistance, and creep resistance. The densities of titanium aluminides are low compared to nickel or iron aluminides (Ref 1-3). Among the titanium aluminides, alloys based on α_2Ti_3Al and γTiAl have received wide attention in recent years. The strong *A-B* bonding of these ordered structures favors the retention of elastic moduli, elastic strength, creep resistance, and fatigue resistance at elevated temperatures due to the slow diffusion kinetics. Many of these ordered structures exhibit anomalous flow behavior, in which the critically resolved shear stress increases then decreases with increasing temperature (Ref 4). Some of the identified applications for these alloys are compressor blades and turbine disks. Gamma titanium aluminides may also find applications as automobile turbo chargers due to their low density of 3.8 g/cc compared to 4.6 g/cc of α_2Ti_3Al alloys (Ref 5).

Like other intermetallic aluminides, titanium aluminides suffer from poor room temperature ductility. Additions of up to 25 at.% niobium to α_2 alloys considerably improved the ductility (Ref 6). The γ alloys that have been developed so far are classified as single-phase γ alloys and two-phase $\alpha_2 + \gamma$ alloys. Single-phase γ alloys contain ternary additions, such as Nb or Ta, that improve the strength and oxidation resistance. In the two-phase alloys, additions of V, Cr, and Mn improve ductility whereas additions of Nb and Ta improve the oxidation resistance (Ref 7).

The nature of the microstructure achieved by the thermomechanical process plays a significant role in controlling the properties. Structures that are obtained, in general, are either lamellar, equiaxed, or a combination of both. In single-phase γ alloys, the presence of approximately 10 vol% of α_2 improves ductility, and a lamellar volume fraction of approximately 0.3 gives reasonable combination of strength, ductility, and high-temperature properties in the two-phase alloys (Ref 3, 8).

Intermetallic aluminides can be processed by both ingot metallurgy and powder metallurgy routes. In the ingot metallurgy route, vacuum arc melting, electron beam melting, and electroslag remelting are commonly used (Ref 9). Rapid solidification, mechanical alloying, and hot isostatic pressing are the powder metallurgy methods. In recent years, powder metallurgy techniques, such as reactive sintering, vacuum hot pressing, extrusion, dynamic compaction, and plasma spraying, were used to process the high-temperature intermetallic aluminides (Ref 10). Powder processing, in general, improves the microstructural homogeneity, minimizes segregation, and permits near net shape forming approaches and processing of composite structures.

The forming of TiAl billets by the ingot metallurgy route is difficult due to the brittleness of the intermetallic phase. To overcome this, products can be made through the powder metallurgy route using either elemental powder or prealloyed powders. In the reactive sintering process, elemental powders in stoichiometric proportion are blended and compacted to form green compacts and then sintered at the desired temperatures. Schafrik (Ref 11) used this blended elemental approach followed by extrusion to produce a bar product. Wang and Dahms (Ref 12) studied the influence of the extrusion ratio on the sin-

S.G. Kumar and **R.G. Reddy,** Department of Chemical and Metallurgical Engineering, University of Nevada, Reno, NV 89557, USA; and **J. Wu** and **J. Holthus,** Materials Science Division, Lawrence Berkeley Laboratories, University of California, Berkeley, CA 94720, USA.

tering behavior of a cold-extruded powder mixture of Ti-48Al. The successful preparation of alloy parts from prealloyed powders depends on the particle shape and size distribution. Gas atomization and plasma rotating electrode processes are some of the methods used to produce prealloyed powders (Ref 10). Titanium has a strong affinity toward hydrogen, forming brittle hydrides. This is the basis for thermochemical processing, which is essentially a hydride-dehydride process. This process refines the final microstructure, which may lead to significantly improved mechanical and fatigue properties (Ref 13). The authors recently presented the refined microstructures obtained through this process in an α_2Ti_3Al alloy and the effect of processing on phase relations in a series of high-temperature aluminides (Ref 14-17). In the present study, a systematic investigation was undertaken to study the effect of powder processing on the microstructure and phase relations in a 44Ti-44Al-12Nb at.% alloy (48Ti-27Al-25Nb wt% alloy). Samples were processed through: (a) cold compaction of elemental powders followed by sintering (CP process); (b) hot vacuum pressing of cold compacted elemental powders followed by sintering (HP process); and (c) arc melting to produce alloy ingot, hydride-dehydride process to make prealloyed powders, cold isostatic pressing, then sintering (AM process). These samples were analyzed by XRD, optical microscopy, SEM-EDS, and EPMA for phase and microstructural analysis.

2. Experimental Procedure

The three processing methods adopted in this study are cold pressing (CP), hot pressing (HP), and arc melting (AM). For the CP and HP studies, samples in 44Ti-44Al-12Nb (at.%) were prepared from elemental powders of –325 mesh size. Titanium powder (99.98% pure), aluminum powder (99.99% pure), and niobium powder (99.8% pure) were used. For AM studies, titanium wires (99.99% pure), aluminum rods (99.999% pure), and niobium chunks (99.95% pure) were used to avoid sputtering of powders.

2.1 *Sample Preparation*

Sample preparation techniques are described in detail elsewhere (Ref 14), and only a brief description is given here. In the CP process, the powders were weighed in stoichiometric proportions, thoroughly mixed in a V-shaped rotating mixer for about five hours, and then compacted into 11.2-mm-diameter pellets using steel die at 396 MPa for one minute. The compacted pellet was then reaction sintered at 1273 K in argon atmosphere.

In the HP process, a cold compacted pellet was prepared in a way similar to the CP process, and the pellet was surrounded by a layer of boron nitride powder on all sides in a graphite die of 12.5-mm inner diameter. The graphite die was placed in a vacuum furnace (10^{-5} atm) and hot pressed at 900 K and 36 MPa for 10 minutes. After hot pressing, the pellet was cleaned on SiC paper followed by ultrasonic cleaning to remove any traces of the boron nitride powder. These pellets were then sintered at 1273 K in argon atmosphere.

In the AM process, which refers to preparation of the alloy from prealloyed powders, the titanium wires and niobium

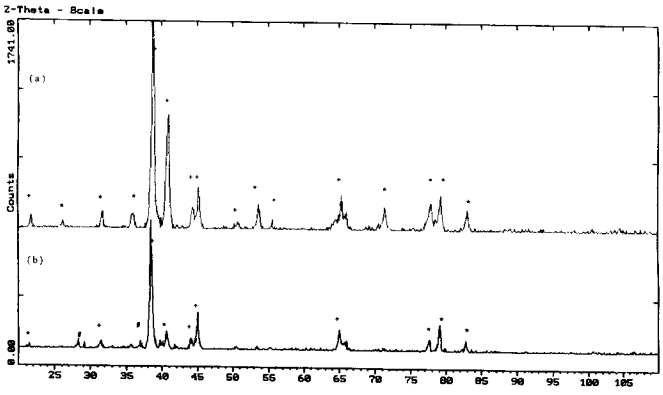

Fig. 1 X-ray analysis of the 44Ti-44Al-12Nb alloy processed through (a) the AM route and (b) the HP route. * indicates Ti_3Al. + indicates TiAl. # indicates Nb_2Al.

chunks were melted repeatedly on a copper hearth under a flow of purified argon gas using tungsten electrodes. Titanium and niobium were melted before the addition of aluminum rods to prevent the evaporation losses of aluminum at the high temperatures and vacuum involved. Aluminum rods were also melted together with Ti-Nb to get a final solidified button of 2.5 grams. Prealloyed powders of –325 mesh size were prepared from this solidified button using the hydride-dehydride process. For this, the arc melted alloy button was crushed into coarse, solid pieces, which were then hydrogenated in hydrogen atmosphere at 1073 K. The coarse powder then was crushed and ball milled for five hours using tungsten carbide balls in hexane solution to prevent oxidation. After ball milling, the solution was filtered out, and the fine alloy powder obtained was dried overnight in open air. The dried powder was dehydrogenated at 1173 K and 10^{-5} atm vacuum for one hour. This powder was sieved to obtain –325 mesh size, which was cold pressed at 612 MPa and cold isostatic pressed at 1296 MPa to obtain 12.5-mm-diameter pellets. The pellets were then sintered at 1273 K.

2.2 *Sintering*

The cold-pressed and hot-pressed pellets were wrapped with tantalum foil and sintered at 1273 K in a high-temperature furnace backfilled with argon gas. To avoid the melting of aluminum in the pellets, the samples were heated up to 873 K, kept at that temperature for 18 hours, and heat treated at 1273 K for 30 hours. For the pellet made from the arc melting route, the sample was directly heated up to 1273 K and maintained there for 18 hours.

3. Results and Discussion

3.1 *XRD*

All three samples were characterized for phase analysis by XRD using a Siemens D500 diffractometer with DIFFRAC AT software (both registered tradenames of Siemens Industrial Automation, Inc., Madison, WI 53719). Also, the powder obtained after hydrogenation of the arc melted sample was analyzed by XRD for hydride formation. The peak positions

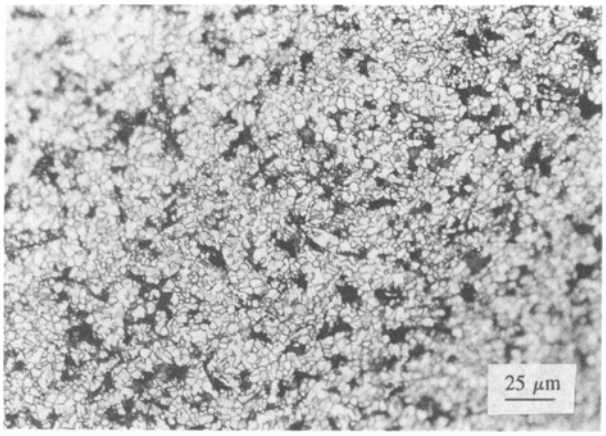

Fig. 2 Microstructure of 44Ti-44Al-12Nb alloy processed through AM.

Table 1 Electron probe microanalysis

Sample	Phase	Composition, at.% Ti	Al	Nb
AM processed	Bulk	43	45	12
HP processed	1	38	49	13
	2	45	50	5
	Nb_2Al	10	36	54

obtained for CP and HP processed samples are quite similar, though CP processed samples exhibited a large background. Figure 1 compares the XRD patterns obtained on the pellets processed by HP and AM processes. Notice that the phases identified are mostly α_2Ti_3Al and $\gamma TiAl$, and some of the peaks in the HP sample correspond to the Nb_2Al phase.

3.2 *Microstructural Features*

After XRD analysis, the samples were mounted and polished to obtain a scratch-free surface using 240, 320, 400, and 600 grit SiC paper. Final polishing was done on microcloth using diamond slurry. The sample surface was then etched with an etchant prepared from 10 mL concentrate HF, 5 mL concentrate HNO_3, and 85 mL H_2O for 15 seconds and observed for microstructural features using an optical microscope. The mi- crostructures of CP and HP processed samples are porous and do not reveal any significant features. The porosity of the CP and HP processed samples is estimated to be approximately 40 to 45% based on the micrographs taken in unetched and etched conditions.The microstructure of an AM processed sample is shown in Fig. 2. The microstructure of the sample processed by the AM route is quite distinct and dense when compared to the other two samples with a porosity of approximately 4 to 6%. The microstructure reveals a dual-phase structure consisting of Ti_3Al islands in a matrix of fine equiaxed TiAl grains. The HP and AM processed samples were then coated with silver and analyzed by a SEM-EDS attachment. Figures 3(a) to (d) and 4(a) to (c) show the SEM micrograph of HP and AM processed samples, respectively, along with the EDS spectra. No clear microstructural morphology is discernible in HP samples as shown in Fig. 3(a). The bulk composition of the sample approximates to initial stoichiometric proportion (Fig. 3b). Some areas revealed the TiAl phase with lower soluble Nb (Fig. 3c) and some Nb-rich phases corresponding to Nb_2Al (Fig. 3d). The equiaxed nature of the AM sample, as shown in Fig. 2, is manifested by the SEM micrograph shown in Fig. 4(a) and (b) at different magnifications. Note the hexagonal nature of some of the grains corresponding to the Ti_3Al phase. This sample, in general, revealed the same composition throughout the matrix (Fig. 4c).

3.3 *EPMA*

The pellets prepared by HP and AM routes were also analyzed by EPMA. The elementary distributions of titanium, aluminum, niobium, and oxygen in an AM sample are shown in Fig. 5. A light field indicates a high content of the element considered. The distribution of the elements is uniform. The elemental mapping of Ti, Al, and Nb in both the samples is shown in Fig. 6(a) to (f). The concentrations in Fig. 6 are in weight percent. These elements are equally distributed throughout the matrix in the AM sample (Fig. 6d-f) while their distribution is nonhomogeneous in the HP sample (Fig. 6a-c) with varying content of 16 to 56 wt% Ti, 8 to 28 wt% Al, and 0 to 20 wt% Nb. The quantitative analysis of these samples is given in Table 1. Only α_2 and γ are present in the AM sample whereas the HP sample has the Nb_2Al phase in addition to α_2 and γ.

4. Discussion

The Ti-Al binary phase diagram indicates a wide range of homogeneity for $\gamma TiAl$ (Ref 18). Alloys with 22 to 36 at.% Al are single-phase Ti_3Al in nature. Those with 36 to 49 at.% Al are two-phase Ti_3Al + TiAl, and those with 49 to 66 at.% Al are single-phase $\gamma TiAl$. In conventional solidification, the formation of $\gamma TiAl$ proceeds by a peritectic reaction between βTi and liquid Ti at approximately 1753 K. The presence and amount of the Ti_3Al phase depends on the exact composition of the alloy. In the present AM process, one would expect the as-cast structure to be lamellar or dendrites of γ and α_2 with γ being the peritectic reaction product. However, the microstructure after final heat treatment does not show the presence of any lamellar structure. The microstructure is predominantly fine equiaxed grains of γ and α_2 phases as detected by XRD. In this context, it is pertinent to discuss the refining effect of hydride-dehydride process on the microstructure. The solubility of hydrogen in $\gamma TiAl$ is very little while it is quite high in Ti_3Al (Ref 7). The substantial refinement of the microstructure after final heat treatment and the brittleness of the alloy after hydrogenation indicates that a large amount of hydrogen has entered the alloy lattice forming brittle titanium hydrides. The presence of titanium hydrides is confirmed by XRD. This in turn confirms the presence of the hcp α_2 phase in the as-cast alloy. This observation is consistent with the results of many investigators, which indicated that the phase that forms from the liquid is not cubic β but the hexagonal phase (Ref 19-21). SEM micrographs of the AM sample revealed the presence of hexagonal shaped

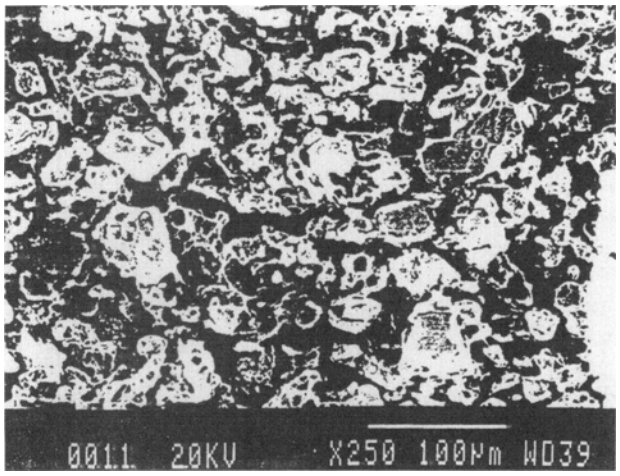

(a)

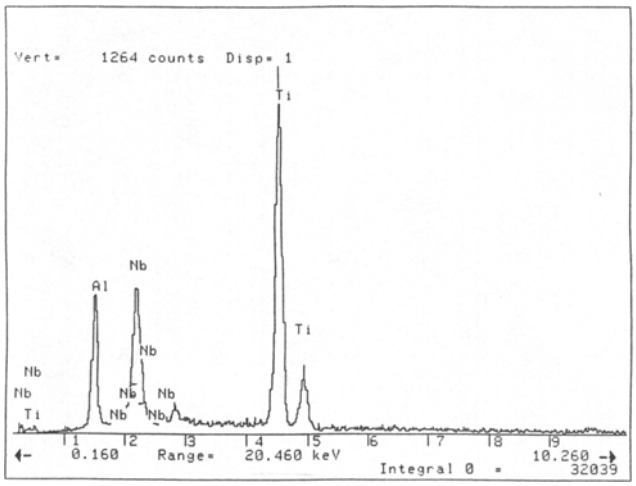

(b)

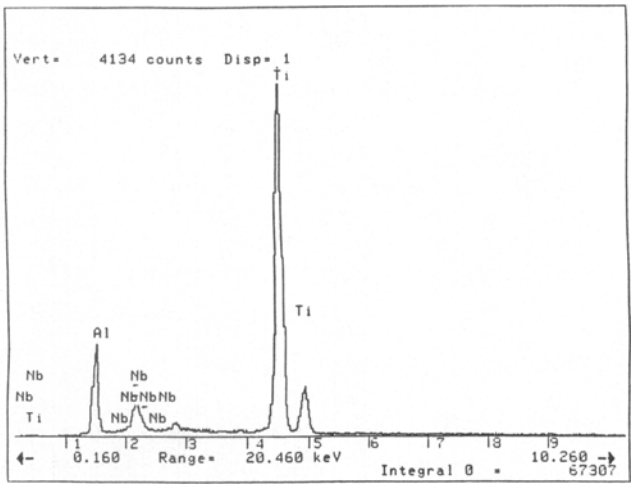

(c)

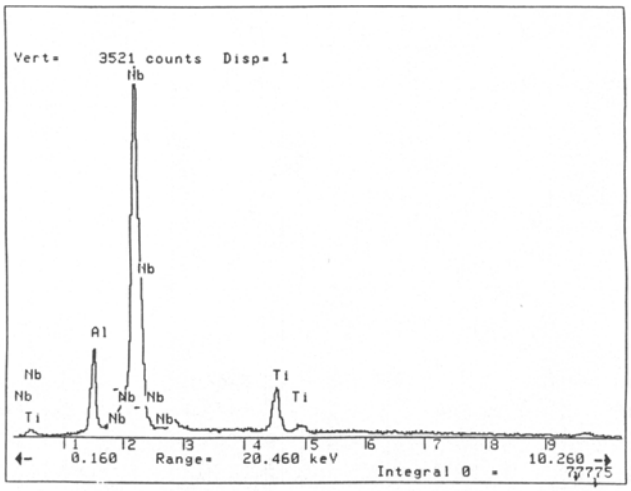

(d)

Fig. 3 SEM-EDS analysis of 44Ti-44Al-12Nb alloy processed by HP. (a) SEM micrograph. (b) EDS spectrum indicating bulk composition. (c) EDS spectrum indicating Ti-rich phase. (d) EDS spectrum indicating Nb-rich phase.

grains (Fig. 4b). The presence of α_2 and γ is confirmed by XRD and is consistent with the reported phases in Ti-Al binary alloys (Ref 12, 19-25). EDS and EPMA data could only confirm the composition to be in stoichiometric proportion, and no clear Ti_3Al and TiAl phases are discernible based on the composition. The elemental mapping indicated that the distribution of phases is uniform, which is consistent with the fine equiaxed microstructure of optical microscopy (Fig. 5).

The forming of a cast TiAl ingot/billet is difficult due to the brittleness of the intermetallic phase. This problem can be overcome by the powder metallurgy approach of cold extrusion followed by reactive sintering. Hot pressing in vacuum helps in achieving the consolidation. The XRD pattern and microstructures obtained in the present study of CP and HP processes are similar. The XRD data indicated peaks corresponding to Ti_3Al, TiAl, and Nb_2Al. The presence of Nb_2Al was confirmed by EDS and EPMA data. In general, these samples are chemically inhomogeneous and porous in nature. The high porosity present in the samples could be due to the low compaction pressures used and to the Kirkendall effect. In the present study, the samples were sintered at 873 K for nearly 18 hours before the final heat treatment of 1273 K for 30 hours. In other words, primary sintering is pure solid state interdiffusion, which leads to the Kirkendall effect in which creation and accumulation of vacancies takes place on the side of the diffusion couple with the faster diffusing constituent (Ref 26). As a result of such one-sided diffusion, the porosity of the previously dense sample increases. The absence of this effect in a Ti_3Al-Nb alloy was noted by the present authors recently (Ref 14). In the HP sample, EPMA data indicated two Ti-Al phases with a large difference in the niobium solubility. The solubility of niobium in α_2Ti_3Al is 12 at.% (Ref 27). Based on this, the phase with 38Ti-49Al-13Nb is identified as Ti_3Al, and the phase with 45Ti-50Al-5Nb is TiAl.

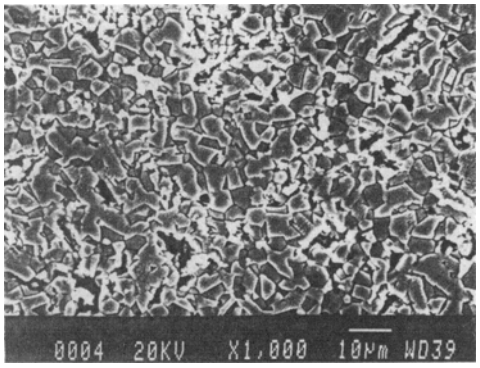

(a)

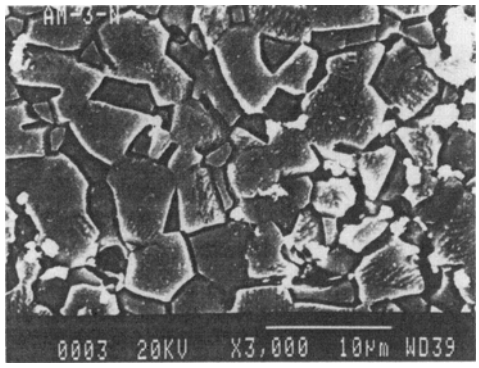

(b)

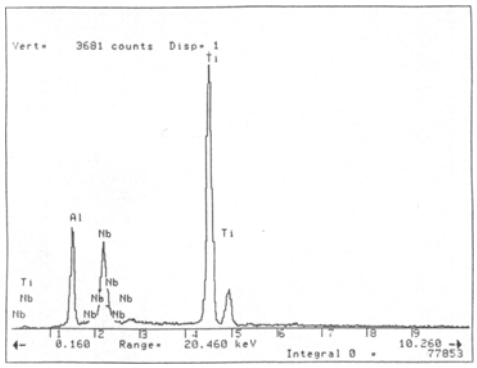

(c)

Fig. 4 **SEM-EDS** analysis of 44Ti-44Al-12Nb alloy processed by AM: (a) and (b) SEM micrograph. (c) EDS spectrum indicating bulk composition.

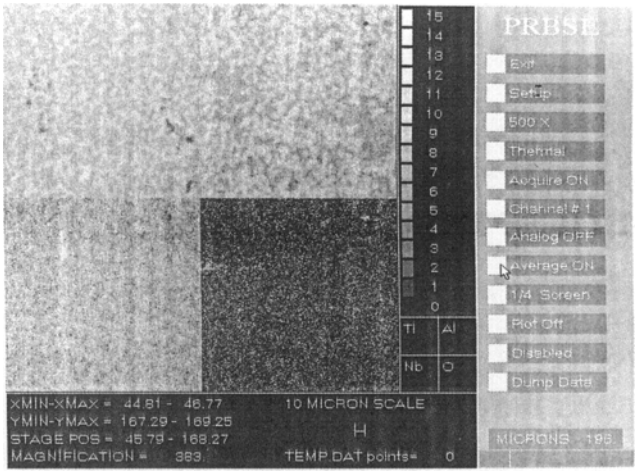

Fig. 5 EPMA mapping of the elemental distribution in the alloy processed by the AM process.

The γTiAl phase is resistant to oxidation up to 1173 to 1273 K compared to the 923 K limit of Ti_3Al alloys (Ref 7). However, the oxidation resistance decreases with decreasing Al content or increasing volume fraction of the α_2 phase. Elements like niobium, tantalum, or tungsten will improve the oxidation resistance. Oxygen is an α stabilizer, and its solubility in α_2Ti_3Al is more when compared to γTiAl. The reported value of the solubility of oxygen in γTiAl is 1500 to 2300 ppm (Ref 11). Oxygen from γTiAl diffuses to the α_2Ti_3Al phase during cooling. Lowering of the oxygen content of the γ phase improves the ductility of γTiAl alloys (Ref 22). The average oxygen content as determined by EPMA is 1375 ppm, varying from 100 to 2500 ppm in the AM sample, and 1500 ppm, varying from 900 to 2500 ppm in the HP sample. Such a large scatter in oxygen values of γTiAl alloys is reported in Ref 28.

5. Conclusions

Intermetallic alloys based on the γTiAl phase are considered to be some of the potential high-temperature structural materials. Currently, research efforts are underway to improve the room temperature ductility of these materials through the additions of various alloying elements. Niobium additions are known to improve the oxidation resistance. These alloys are processed by either the ingot metallurgy route of melting and casting or the powder metallurgy route of rapid solidification, hot isostatic pressing, etc. All these methods need high temperatures and pressures. The present study was undertaken to develop an alternative, cost-effective powder metallurgy processing of these materials. A Ti-Al-Nb intermetallic alloy with the composition 44-44-12, respectively, was processed by the powder metallurgy route of alloy preparation from elemental powders (CP and HP processes) and prealloyed powders (AM

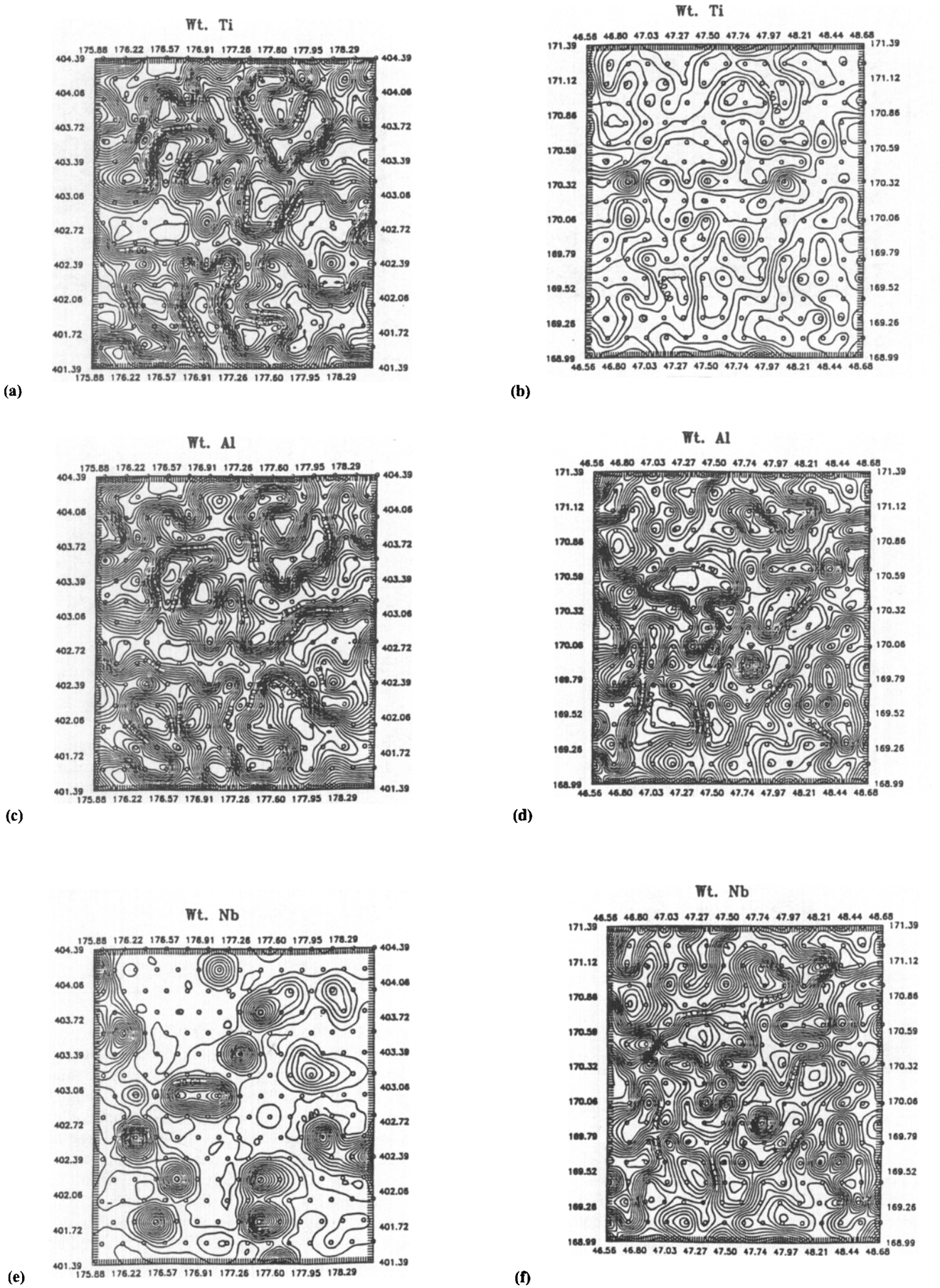

Fig. 6 Quantitative elemental distribution of Ti, Al, and Nb. (a)-(c) HP process. (d)-(f) AM process.

process). The CP process refers to the reactive sintering of cold compacted powders, and the HP process is sintering of hot vacuum pressed powders. In the AM process, the prealloyed powders are made using the hydride-dehydride process of arc-melted button ingots. Phase analysis carried out by XRD, EDS, and EPMA indicated the presence of Ti_3Al and TiAl in both HP and AM samples and Nb_2Al in the HP sample. Microstructural evaluation revealed that CP and HP processed samples are porous and chemically inhomogeneous whereas the AM process resulted in a dense sample with fine equiaxed grains of α_2Ti_3Al and γTiAl. This refinement of microstructure is attributed to the thermomechanical processing step of the hydride-dehydride process. Based on the experimental study, the processing of TiAl-Nb ternary alloys through the AM route gives better results.

Acknowledgments

Two of the authors, S.G.K. and R.G.R, are pleased to acknowledge the financial support of this research by National Science Foundation, grant No. DMR-9314016. The authors are grateful to Professor L. Brewer of Lawrence Berkeley Laboratories for his encouragement through the course of this research.

References

1. W.B. Pearson, *A Handbook of Lattice Spacings and Structures of Metals and Alloys*, Vol 2, Pergamon Press, 1967, p 126
2. J.R. Groza, S.H. Risbud, and K. Yamazaki, *Proc. Plasma Synthesis and Processing of Materials*, K. Upadhya, Ed., TMS, 1993, p 85-93
3. F.H. Froes, C. Suryanarayana, and D. Elizer, *J. Mater Sci.*, Vol 27, 1992, p 5113-5140
4. D.P. Pope, *Proc. High Temperature Aluminides and Intermetallics*, S.H. Whang, C.T. Liu, D.P. Pope, and J.O. Stiegler, Ed., TMS, 1992, p 51-61
5. Y. Nishiyama, T. Miyashita, S. Isobe, and T. Noda, *Proc. High Temperature Aluminides and Intermetallics*, S.H. Whang, C.T. Liu, D.P. Pope, and J.O. Stiegler, Ed., TMS, 1991, p 557-584
6. R.G. Rowe, *Adv. Mater Proc.*, Vol 141 (No. 3), 1992, p 33
7. Y.W. Kim, *J. Met.*, July 1989, p 24-30
8. T. Tsujimoto and K. Hashimoto, *Proc. High Temperature Ordered Intermetallic Alloys III*, Vol 133, C.T. Liu, A.I. Taub, N.S. Stoloff, and C.C. Koch, Ed., MRS, 1989, p 391-396
9. S.G. Kumar and R.G. Reddy, *Proc. Extractive Metallurgy of Copper, Nickel and Cobalt*, R.G. Reddy and R.N. Weizenbach, Ed., TMS, 1993, p 1101-1123
10. J.H. Moll, C.F. Yolton, and B.J. McTiernan, *Int. J. Powder Metall.*, Vol 26 (No. 2), 1990, p 149-155
11. R.E. Schafrik, *Metall. Trans. B*, Vol 7, 1976, p 713-716
12. G.-X. Wang and M. Dahms, *Metall. Trans. A*, Vol 24, 1993, p 1517-1526
13. F.H. Froes, D. Eylon, and C. Suryanarayana, *JOM*, Vol 42 (No. 3), 1990, p 26
14. S.G. Kumar and R.G. Reddy, unpublished research
15. R.G. Reddy and K.N. Hebbar, *Proc. Electron Beam Melting and Refining—State of the Art 1991*, R. Bakish, Ed., Bakish Materials Corporation, 1991, p 248-291
16. D.M. Kocherginsky and R.G. Reddy, *Proc. Control of Interfaces in Metal and Ceramic Composites, R.Y. Lin and S.G. Fishman*, Ed., TMS, 1994, p71-79
17. S.G. Kumar, R.G. Reddy, and L. Brewer, *J. Phase Equilibria*, Vol. 15 (No. 3), June 1994, p. 279-284
18. U.R. Kattner, J.-C. Lin, and Y.A. Chang, *Metall. Trans. A*, Vol 23, 1992, p 2081
19. J.A. Graves, J.H. Perepezko, C.H. Ward, and F.H. Froes, *Scr Metall.*, Vol 21, 1987, p 567-572
20. J.J. Valencia, C. McCullough, C.-G. Levi, and R. Mehrabian, *Scr Metall.*, Vol 21, 1987, p 1341-1346
21. G.E. Fuchs and S.Z. Hayden, *Mater Sci. Eng. A*, Vol 152, 1992, p 277-282
22. T. Kawabata, T. Tadano, and O. Izumi, *Scr Metall.*, Vol 22, 1988, p 1725-1730
23. P. Prasad Rao and K. Tangri, *Mater Sci. Eng. A*, Vol 132, 1991, p 49-59
24. C.R. Feng, D.J. Michel, and C.R. Crowe, *Mater Sci. Eng. A*, Vol 145, 1991, p 257-264
25. S. Yamauchi and H. Shiraishi, *Mater Sci. Eng. A*, Vol 152, 1992, p 283-287
26. F.V. Lenel, *Powder Metallurgy: Principles and Applications*, Metal Powder Industries Federation, 1980
27. J.H. Perepezko, Y.A. Chang, L.E. Seitzman, J.C. Lin, N.R. Bonda, T.J. Jewett, and J.C. Mishurda, *Proc. High Temperature Aluminides and Intermetallics*, S.H. Whang, C.T. Liu, D.P. Pope, and J.O. Stiegler, Ed., TMS, 1991, p 19-47
28. C. Suryanarayana, G.-H. Chen, A. Frefer, and F.H. Froes, *Mater Sci. Eng. A*, Vol 158, 1992, p 93-101